CONTINUUM POLARIZATION IN MAGNETIC WHITE DWARFS*

F. K. LAMB
Dept. of Physics, University of Illinois, Urbana, Ill. 61801, U.S.A.
and
P. G. SUTHERLAND
Dept. of Physics, Columbia University, New York, N.Y. 10027, U.S.A.

Abstract. We discuss some of the effects which magnetic fields in the range 10^4–10^8 G have on the continuum emission of white dwarfs. In order to show how atomic processes are related to the transport of radiation in an anisotropic medium we introduce the radiative transfer equation for polarized light. Using this transfer equation as a guide we develop a greatly simplified model of a white dwarf atmosphere: anisotropic absorption of unpolarized light passing through a cold, optically-thin layer. Two possible sources of continuum polarization in white dwarfs with strong magnetic fields are explored, namely bound-free transitions and cyclotron absorption. Within the hydrogenic approximation we develop a further approximation which is valid for bound-free transitions when B is in the range 10^4–10^7 G. Using this approximation it is possible to obtain simple expressions for the net circular and linear polarization in terms of the zero-field opacity. In the case of cyclotron absorption, the cross section is large and strongly peaked at the cyclotron frequency, which falls in the infrared or optical for $B \geqslant 10^8$ G. This process can lead to net circular and linear polarization of comparable magnitude. For stars with non-uniform magnetic fields, the cyclotron absorption effects are spread over considerable wavelength ranges, with possibly quite complicated wavelength-dependent polarization.

1. Introduction

In the past three years there has been growing interest in the possible existence of white dwarfs with strong magnetic fields. A number of authors (Ostriker and Hartwick, 1968; Ginzburg *et al.*, 1969; Chow, 1969) have noted that application of the same argument put forward to explain the apparently large magnetic fields in pulsars – namely, conservation of flux in the compression of a normal star to a neutron star in a supernova – would suggest magnetic fields of the order of 10^6–10^7 G. The process by which white dwarfs are formed is unclear, however, and the extent to which this scaling argument applies is uncertain. Nevertheless, conjectures of this kind have stimulated a number of observational searches for evidence of strong magnetic fields in white dwarfs.

Three approaches have been used: examination of the wings of hydrogen lines for circular polarization due to the linear Zeeman splitting of the unperturbed line (Angel and Landstreet, 1970a), interpretation of residual displacements of hydrogen lines in terms of the quadratic Zeeman effect (Preston, 1970; Trimble, 1971; see also Lamb and Sutherland, 1971, for further discussion of this problem), and measurements of continuum circular polarization with broad pass-band filters (Angel and Landstreet,

* Presented by P. G. Sutherland.

C. J. Hansen (ed.), Physics of Dense Matter, 265–285.

1970b, 1971a, b; Landstreet and Angel, 1971; Kemp *et al.*, 1970; Kemp and Swedlund, 1970; Kemp *et al.*, 1971; and Gehrels, 1971) and multichannel photospectrometers (Angel *et al.*, 1972a, b; Angel and Landstreet, 1972). The first two approaches were confined exclusively to the DA white dwarfs and led to upper limits on the magnetic field strengths in DA stars of about 10^5 G.

The most successful search method to date has been the search for circular polarization in the continuum radiation; the data for four stars, Grw+70°8247, G99-37, G195-19, and G99-47, have been published. Grw+70°8247 is a 'peculiar' white dwarf, famous for its unassigned Minkowski bands (see Greenstein and Matthews, 1957; Greenstein, 1970; and Angel, 1972 for tentative assignments), the most notable one being at λ4135. From the trigonometric parallax and a black-body interpretation of the $U-B$, $B-V$ colors, the temperature is near $T_e = 11\,500$ K and the radius is near $0.012\,R_\odot$ (Greenstein and Matthews, 1957). In Figure 1 we give the data for the net circular and linear polarizations, for wavelengths between λ3000 and λ11 000, taken from the work of Angel *et al.* (1972b) and the work of Angel and Landstreet (1970b). The most striking features of the data are the rapid decrease and increase of the circular polarization in the λ3000–4000 range, the slow decrease of the circular polarization with increasing wavelength above λ4000, and the large linear polarization near λ4000. There are also dramatic changes in the circular polarization in the vicinity of the Minkowski bands; a possible interpretation of these latter results has been put forward by Angel (1972). The second magnetic white dwarf, G99–37, is a λ4670p star with CH band heads near $\lambda\lambda$3880, 4300 and the Swan bands of C_2 near

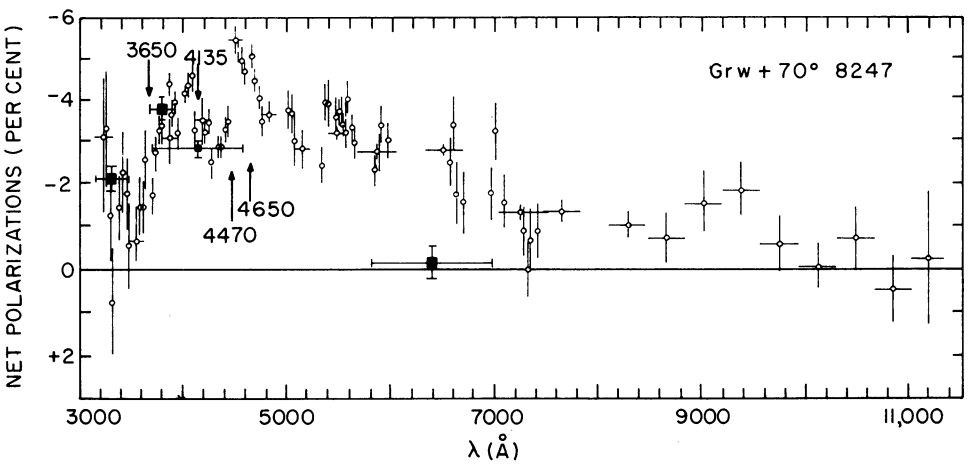

Fig. 1. The net circular and linear polarizations versus wavelength for the white dwarf Grw + 70°8247. The round dots indicate circular polarization and are taken from a graph given by Angel *et al.* (1972b); the square dots at $\lambda\lambda$3300, 3800, 4150, and 6400 indicate linear polarization and are taken from a graph given by Angel and Landstreet (1970b). The circular polarization measurements were made with a multichannel spectrophotometer and the linear polarization measurements were made with filters; the horizontal error bars correspond to the channel and filter widths, and the vertical error bars represent observational uncertainties. The vertical arrows indicate the positions of the 'Minkowski' bands that are prominent in the spectrum.

λλ4380, 4680, 5170 (Landstreet and Angel, 1971; Greenstein, 1970; Greenstein *et al.*, 1971). The polarization data for G99-37 are given in Figure 2 (the positions of the molecular absorption features are indicated by vertical arrows), taken from Landstreet and Angel (1971). These data differ markedly from the Grw + 70° 8247 data: the average circular polarization is considerably smaller (0.63% compared with 3.5%), and the ratio of linear to circular polarization is very small. The data for the third magnetic white dwarf, G195-19, a DC star, are similar to those of G99-37, with circular polarization ~0.22% and no detectable linear polarization (Angel and Landstreet, 1971a, b; Angel *et al.*, 1972a). In contrast to the previous two stars, the polarization of G195-19 was found to be time-varying with an amplitude of 0.25% and a period of 1.339 days, presumably due to rotation. Hence the published data, which were taken at different phases, only give a rough idea of the wavelength dependence of the polarization. The fourth magnetic white dwarf, G99-47, shows circular polarization ~0.4% and no detectable linear polarization (Angel and Landstreet, 1972). Recent observations of G99-37 by Angel and Landstreet, with improved sensitivity and resolution, have revealed a classical molecular linear Zeeman pattern at the CH λ4300 band head; with 160 Å resolution the circular polarization jumps through ~6% across the band head, indicative of a magnetic field strength $\gtrsim 10^6$ G (Angel, private communication). This observation is perhaps the single most convincing piece of evidence that

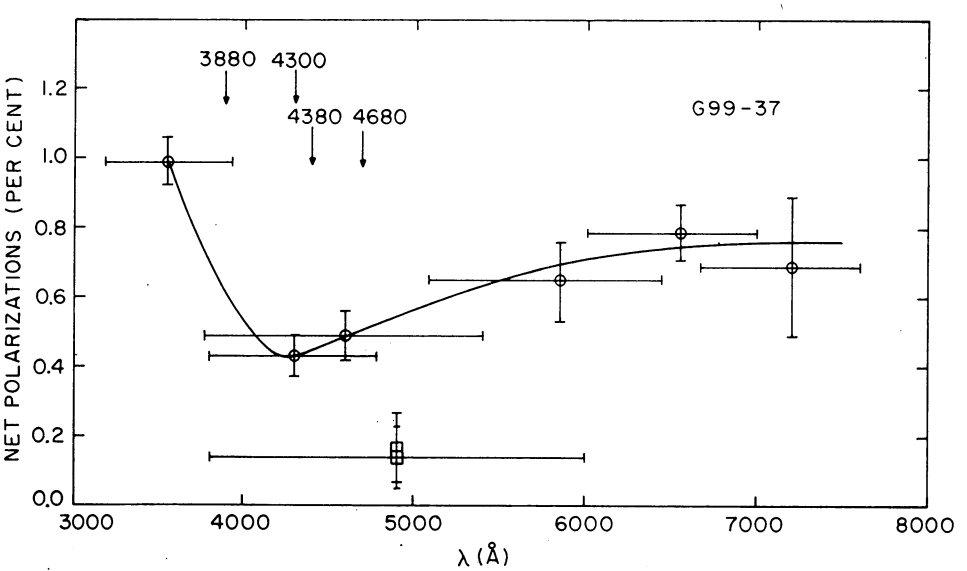

Fig. 2. The net circular and linear polarizations versus wavelength for the white dwarf G99-37, adapted from a graph given by Landstreet and Angel (1971). The round dots indicate circular polarization measurements; the curve drawn through these points is meant only to guide the eye. The two linear polarization measurements, indicated by the square dots, were made in two perpendicular directions. The horizontal error bars correspond to the filter widths and the vertical error bars represent observational uncertainties. The two vertical arrows at λλ3880, 4300 indicate the positions of band heads in CH and the two vertical arrows at λλ4380, 4680 indicate the Swan bands of C_2; these are prominent absorption features in the spectrum.

https://doi.org/10.1017/S0074180900100075 Published online by Cambridge University Press

the polarizations in these four white dwarfs are in fact due to magnetic fields.

The measurements of the continuum polarizations have been interpreted using the grey-body model (Kemp, 1970a, b; see also Shipman, 1971; Chanmugam *et al.*, 1972). This model may give an order-of-magnitude estimate of the field strengths but does not agree in detail with the data. One reason for this is the assumed grey-body character of the opacity: for $\Omega_L \ll \omega$ this leads to circular polarization proportional to Ω_L/ω where $\Omega_L = eB/2mc$ is the electron Larmor frequency and ω is the angular frequency of the light. In this approximation the linear polarization is proportional to $(\Omega_L/\omega)^2$. This model almost certainly fails for Grw+70°8247, where, as mentioned above, the linear and circular polarization are comparable and $\sim 4\%$ at $\lambda 4000$. Using the grey-body model, the field strengths for G99-37 and G195-19 are estimated to be roughly 3×10^6 G and 10^6 G, respectively.

To conclude this brief survey of magnetic white dwarfs several remarks are in order. First, only four of approximately sixty white dwarfs examined were found to show detectable polarization, indicating magnetic fields greater than 10^5 G; thus the fraction of white dwarfs with magnetic fields as large as this is apparently small. Second, even among the four white dwarfs which show polarization there appears to be a considerable spread in indicated field strengths: as mentioned above, both the linear and circular polarization in Grw+70°8247 are an order of magnitude greater than the measured circular polarization in the other three, which show no detectable linear polarization. Given this context and the rather long and complex evolutionary processes which are thought to lead to white dwarf formation, use of the flux conservation model to account for magnetic fields in white dwarfs leaves unexplained at least as much as it explains.

In Section 2 we discuss the transfer equation for polarized radiation in an anisotropic medium (the anisotropy, in this case, is provided by the magnetic field). The effects of transfer on the polarization of radiation emerging from a plane-parallel semi-infinite atmosphere are briefly discussed. In cases where the characteristic states of the semi-infinite medium are orthogonal we show that Faraday rotation does not affect the polarization of the emerging radiation so that the polarization is determined by the absorption matrix alone. We then obtain the form of the absorption matrix when the absorption is due to electric dipole transitions (as is the case for those opacity sources discussed in Sections 3 and 4). To illustrate the principal polarization features that may arise, we examine a very simple model: a cold, optically thin layer through which initially unpolarized radiation passes and acquires polarization due to the anisotropic absorption.

Section 3 discusses bound-free absorption by hydrogenic atoms (specifically hydrogen and helium) in a magnetic field. Within the hydrogenic approximation we develop a further approximation which is valid for field strengths in the range 10^4–10^7 G. Using this approximation and the results of Section 2, it is possible to obtain simple expressions for the net circular and linear polarizations in terms of the zero-field opacity. We find that, away from absorption edges, the hydrogenic bound-free opacity gives the same field strength and frequency dependence as the grey-body model. How-

ever, near an absorption edge the opacity is discontinuous and the polarization undergoes sudden changes in sign and magnitude. If hydrogen-like bound-free processes form a significant source of opacity in white dwarfs with magnetic fields of order 10^7 G, characteristic polarization features should be observable near absorption edges.

In Section 4 we briefly consider polarization due to cyclotron absorption. This process is of particular interest for stars which show strong linear as well as circular polarization (such as Grw+70°8247), since it can lead to net circular and linear polarizations of comparable magnitude. The cyclotron absorption cross section is large and strongly peaked at the cyclotron frequency. The magnetic field in a typical white dwarf atmosphere is almost certainly not constant in either direction or magnitude over the surface of the star; averaging over the surface field will spread the cyclotron absorption features over broad wavelength ranges. These features occur in the infrared and optical for $B \gtrsim 10^8$ G.

2. The Transfer Equation for Polarized Radiation

In this section we formulate the radiative transfer equation for polarized light. The passage of polarized light through an anisotropic medium can be conveniently treated in terms of the two characteristic polarization states defined at each point in the medium. Light of either of these two polarization states, which are generally not orthogonal, propagates locally within the medium with its own particular complex refractive index. Providing the properties of the medium change only over distances much larger than the wavelength of the light, at each point in the medium light of arbitrary polarization can be resolved into components using as a basis the characteristic states of the medium at that point and the absorption and propagation of each component can then be followed separately. This approach is discussed in considerable detail by Lamb and ter Haar (1970); below we summarize the main results.

In order to describe the polarization properties of the light, we shall introduce a polarization matrix, analogous to the density matrix ordinarily used in quantum mechanics; rules for obtaining the corresponding values of the Stokes parameters from this polarization matrix are given in the Appendix. The radiative transfer equation can then be written in terms of a transfer matrix $\mathscr{T}$ and an emission matrix $\mathscr{E}$. The eigenvectors of $\mathscr{T}$ correspond to the characteristic polarization states of the medium; in the basis composed of these eigenvectors the explicit form of $\mathscr{T}$ is readily obtained. (We are primarily concerned here with continuum polarization, therefore we shall not discuss the effects of line emission and absorption although they may be included in a relatively straightforward way – see Lamb and ter Haar, 1970.)

Consider the local propagation of light at point $\mathbf{r}$ in an anisotropic medium. At the point $\mathbf{r}$ we establish a right-handed Cartesian triplet of unit vectors such that the light is propagating along the 3-direction. The two transverse unit vectors are $\hat{e}_1$ and $\hat{e}_2$; distance along the direction of propagation will be denoted by s. We denote by $\hat{\mathscr{E}}_\pm$ the local characteristic polarization vectors of the medium. The electric induction

https://doi.org/10.1017/S0074180900100075 Published online by Cambridge University Press

vector for light of one of these characteristic polarizations propagates according to

$$\mathbf{D}_{\pm}(\delta s) = |\mathbf{D}_{\pm}(0)|\,\hat{\mathscr{E}}_{\pm} e^{ik_{\pm}\delta s - \mathscr{K}_{\pm}\delta s/2 - 2\pi i\nu t}, \tag{1}$$

where ν is the frequency of the light. We introduce the polarization matrix $\mathscr{I}$ for the light as follows: a light ray of induction vector $\mathbf{D}(s) = D_+(s)\,\hat{\mathscr{E}}_+ + D_-(s)\,\hat{\mathscr{E}}_-$ contributes to the polarization matrix a term

$$\mathscr{I}(s) \equiv \begin{pmatrix} \mathscr{I}_+(s) & \mathscr{I}_\times(s) \\ \mathscr{I}_\times^*(s) & \mathscr{I}_-(s) \end{pmatrix} = \begin{pmatrix} |D_+(s)|^2 & D_+(s)\,D_-^*(s) \\ D_-(s)\,D_+^*(s) & |D_-(s)|^2 \end{pmatrix}. \tag{2}$$

We suppose that the characteristic vectors are related to the Cartesian unit vectors by the transformation

$$\begin{aligned} \hat{\mathscr{E}}_\sigma &= \Sigma_\alpha \hat{e}_\alpha \mathscr{U}_{\alpha\sigma} \\ \hat{e}_\alpha &= \Sigma_\beta \hat{\mathscr{E}}_\beta \mathscr{U}_{\beta\alpha}^{-1}; \end{aligned} \tag{3}$$

$\mathscr{U}$ will not be unitary unless the characteristic vectors are orthogonal. The relationship between the polarization matrices in the characteristic basis, $\mathscr{I}$, and in the Cartesian basis, $\mathscr{I}^{(c)}$, is

$$\begin{aligned} \mathscr{I}^{(c)} &= \mathscr{U}\mathscr{I}\mathscr{U}^\dagger \\ \mathscr{I} &= \mathscr{U}^{-1}\mathscr{I}^{(c)}\mathscr{U}^{-1\dagger}; \end{aligned} \tag{4}$$

this transformation is not a similarity transformation unless $\mathscr{U}$ is unitary. The Stokes parameters of the radiation are obtained from $\mathscr{I}^{(c)}$, and rules for the determination of these are given in the Appendix. Although the approach presented in this section is quite general we shall restrict our considerations to atmospheres in which the characteristic states do not change along the direction of propagation.

The transfer equation for the polarization matrix $\mathscr{I}$ is

$$\frac{\mathrm{d}\mathscr{I}}{\mathrm{d}s} = -\tfrac{1}{2}(\mathscr{T}\mathscr{I} + \mathscr{I}\mathscr{T}^\dagger) + \mathscr{E}, \tag{5}$$

where $\mathscr{E}$ is the emission matrix (its form in LTE will be determined below) and $\mathscr{T}$ is the transfer matrix obtained by substituting (1) into (2) and differentiating:

$$\mathscr{T} \equiv -2i\mathscr{R} + \mathscr{K} = -2i\begin{pmatrix} k_+ & 0 \\ 0 & k_- \end{pmatrix} + \begin{pmatrix} \mathscr{K}_+ & 0 \\ 0 & \mathscr{K}_- \end{pmatrix}. \tag{6}$$

The matrix $\mathscr{K}$ represents, of course, the absorption of light; the matrix $\mathscr{R}$ contains the real parts of the refractive indices and provides for such effects as Faraday rotation.

The form of the emission matrix in LTE may be determined as follows. In a *homogeneous* (but possibly anisotropic) medium in thermodynamic equilibrium we must have $\mathrm{d}\mathscr{I}/\mathrm{d}s = \mathscr{O}$ and the light must be unpolarized black-body radiation. In the

https://doi.org/10.1017/S0074180900100075 Published online by Cambridge University Press

Cartesian basis the latter condition may be written

$$\mathscr{I}^{(c)} = \tfrac{1}{2}B(T)\begin{pmatrix}1 & 0\\ 0 & 1\end{pmatrix}, \qquad B(T) = \frac{2h\nu^3}{c^2}\frac{1}{e^{h\nu/kT}-1}, \tag{7}$$

or in the characteristic basis

$$\mathscr{I} = \mathscr{U}^{-1}\mathscr{I}^{(c)}_{\epsilon}\mathscr{U}^{-1\dagger} \equiv \tfrac{1}{2}B(T)\,\Omega, \tag{8}$$

where $\Omega = \mathscr{U}^{-1}\mathscr{U}^{-1\dagger}$. From the condition $\mathrm{d}\mathscr{I}/\mathrm{d}s = \mathscr{O}$ it follows that

$$\mathscr{E} = \tfrac{1}{2}B(T)\left[(\mathscr{K}\Omega + \Omega\mathscr{K})/2 - i(\mathscr{R}\Omega - \Omega\mathscr{R})\right]. \tag{9}$$

But $\mathscr{E}$ is determined entirely by the local properties of the medium, and hence in LTE is given by (9) even when the medium is inhomogeneous. Note that when the characteristic states are orthogonal, Ω is the unit matrix and $\mathscr{E}$ has the familiar form $\mathscr{E} = \tfrac{1}{2}B(T)\,\mathscr{K}$.

Quite generally we may write $\mathscr{U}$ in the form

$$\mathscr{U} = \begin{pmatrix}a & b\\ b & a\end{pmatrix}. \tag{10}$$

with a, b complex and $|a|^2 + |b|^2 = 1$. Then

$$\Omega = \frac{1}{1-\eta^2}\begin{pmatrix}1 & \eta\\ \eta & 1\end{pmatrix} \tag{11}$$

with $\eta = -2\,Re\,a^*b$; η is a direct measure of the nonorthogonality of the characteristic states. In terms of the matrix components of $\mathscr{I}$, the transfer equation becomes

$$\begin{aligned}\frac{-\mathrm{d}\mathscr{I}_{\pm}}{\mathrm{d}s} &= \mathscr{K}_{\pm}\left[\mathscr{I}_{\pm} - \tfrac{1}{2}\frac{1}{1-\eta^2}B(T)\right]\\ \frac{-\mathrm{d}\mathscr{I}_{\times}}{\mathrm{d}s} &= (\bar{\mathscr{K}} - i\Delta)\left[\mathscr{I}_{\times} - \tfrac{1}{2}\frac{\eta}{1-\eta^2}B(T)\right]\end{aligned} \tag{12}$$

with $\bar{\mathscr{K}} \equiv (\mathscr{K}_+ + \mathscr{K}_-)/2$ the average absorption coefficient and $\Delta \equiv k_+ - k_-$.

The transfer equations for the $\mathscr{I}_+$ and $\mathscr{I}_-$ components of the polarization matrix have the standard form: there is an absorption term and an emission term, the latter being given [apart from a nonorthogonality factor $(1-\eta^2)^{-1}$] by the Planck function. On the other hand, the transfer equation for $\mathscr{I}_\times$ involves a complex absorption term, $(\bar{\mathscr{K}} - i\Delta)\mathscr{I}_\times$, and a 'weak' source function, $\tfrac{1}{2}(\eta/1-\eta^2)B(T)$ (weak if $[1 + \Delta^2/\bar{\mathscr{K}}^2]^{1/2} \times \eta \ll 1$).

If the polarization states are orthogonal ($\eta = 0$), (12) reduces to

$$\begin{aligned}\frac{-\mathrm{d}\mathscr{I}_{\pm}}{\mathrm{d}s} &= \mathscr{K}_{\pm}\left[\mathscr{I}_{\pm} - \tfrac{1}{2}B(T)\right]\\ \frac{-\mathrm{d}\mathscr{I}_{\times}}{\mathrm{d}s} &= (\bar{\mathscr{K}} - i\Delta)\,\mathscr{I}_{\times}.\end{aligned} \tag{13}$$

https://doi.org/10.1017/S0074180900100075 Published online by Cambridge University Press

In this case, the components $\mathscr{I}_{\pm}$ at the boundary of a semi-infinite plane-parallel atmosphere are determined only by the absorption matrix and the run of temperature in the atmosphere: the matrix $\mathscr{R}$ has no effect. Furthermore, the off-diagonal component $\mathscr{I}_{\times}$ will be zero at the boundary because the $\mathscr{I}_{\times}$ transfer equation has an absorption term but no source term. Faraday rotation effects are associated with Δ; in the case of a semi-infinite plane-parallel atmosphere with orthogonal characteristic states Faraday rotation does not affect the polarization of the emerging radiation because of the attenuation of the off-diagonal elements of the polarization matrix.

If the characteristic polarization states are nearly orthogonal ($[1+\Delta^2/\bar{\mathscr{K}}^2]^{1/2}\,\eta \ll 1$) then we may to first order in η ignore the effects of the matrix $\mathscr{R}$ in determining the polarization properties of the emergent radiation. The characteristic states are then just the eigenvectors of the absorption matrix, and in the case of electric dipole transitions these may be determined by symmetry considerations. The absorption matrix is easily expressed in the Cartesian basis; in what follows we shall work exclusively in that basis and drop the superscript c on $\mathscr{I}^{(c)}$.

Deep within the atmosphere of a magnetic white dwarf we expect the light to be essentially unpolarized black-body radiation; it is only as the light diffuses outward through the atmosphere that polarization can develop. In order to explore the qualitative features of the polarization produced by electric dipole absorption in the approximation under discussion, we consider a greatly simplified model of a white dwarf atmosphere in which the following assumptions have been made: (i) absorption takes place in a cold layer of thickness δs where $\bar{\tau}=\bar{\mathscr{K}}\delta s \ll 1$, (ii) the light incident on that absorption layer is unpolarized, and (iii) the magnetic field is homogeneous throughout the layer. Thus below the layer the polarization matrix is*

$$\mathscr{I}(0) = \tfrac{1}{2}\mathscr{I}_{\text{net}}\begin{pmatrix}1 & 0\\ 0 & 1\end{pmatrix} \tag{14}$$

and emerging from the layer it is

$$\begin{aligned}\mathscr{I}(\delta s) &= \mathscr{I}(0) - \tfrac{1}{2}[\mathscr{K}\mathscr{I}(0) + \mathscr{I}(0)\mathscr{K}]\,\delta s\\ &= \tfrac{1}{2}\mathscr{I}_{\text{net}}\left[\begin{pmatrix}1 & 0\\ 0 & 1\end{pmatrix} - \begin{pmatrix}\mathscr{K}_{11} & \mathscr{K}_{12}\\ \mathscr{K}^{*}_{12} & \mathscr{K}_{22}\end{pmatrix}\delta s\right].\end{aligned} \tag{15}$$

The Stokes parameters of the emergent radiation (see the Appendix) are given by

$$S_i = -\tfrac{1}{2}\delta s\,\mathrm{tr}\,(\sigma_i\mathscr{K}) \qquad i = 1, 2, 3. \tag{16}$$

We now turn to an evaluation of the matrix elements of $\mathscr{K}$, in situations where the opacity is determined by electric dipole transitions. To be explicit, we consider that the anisotropy of the atmosphere is due to a uniform magnetic field oriented along the z-axis. If the outward normal to the atmosphere (and also the direction of light propagation) is given by the unit vector

$$\hat{k} = (\sin\theta\cos\phi,\ \sin\theta\sin\phi,\ \cos\theta), \tag{17}$$

* This choice of polarization matrix below the 'reversing-layer' means that Faraday rotation does not affect the polarization of the emerging radiation, just as in the case of the semi-infinite atmosphere.

https://doi.org/10.1017/S0074180900100075 Published online by Cambridge University Press

then we may take the two transverse vectors $\hat{e}_1$ and $\hat{e}_2$, which together with $\hat{k}$ form our basic Cartesian triplet, to be

$$\begin{aligned}\hat{e}_1 &= (\sin\phi, -\cos\phi, 0)\\ \hat{e}_2 &= (\cos\theta\cos\phi, \cos\theta\sin\phi, -\sin\theta).\end{aligned} \tag{18}$$

Now the absorption coefficient, in the dipole approximation, for the absorption of a photon of frequency $\nu = \omega/2\pi$ and polarization $\hat{\mathscr{E}}$ is proportional to the absorption cross section

$$\frac{4\pi^2 e^2 \omega}{c} \sum_{i,f} |\langle f|\, \mathbf{d}\cdot\hat{\mathscr{E}}\, |i\rangle|^2\, \delta(E_f - E_i - \hbar\omega) \tag{19}$$

where E_i, E_f are respectively the energies of the initial and final states of the absorbing system, and $\mathbf{d}$ is the dipole operator. Because the magnetic field (along the $\hat{z}$-axis) tends to break the magnetic quantum number degeneracies in atomic states, it is convenient to express $\mathbf{d}$ as follows:

$$\mathbf{d} = \sum_q \hat{\varepsilon}_q^* d_q \qquad q = \pm 1, 0$$

with

$$\hat{\varepsilon}_\pm = \mp\frac{1}{\sqrt{2}}(\hat{x} \pm i\hat{y}) \qquad \hat{\varepsilon}_0 = \hat{z}\,; \tag{20}$$

d_q can only connect atomic states whose magnetic quantum numbers differ by q. We define three absorption coefficients K_q corresponding to the polarizations $\hat{\mathscr{E}} = \hat{\varepsilon}_q$ in (19); the $\hat{\varepsilon}_q$ and K_q are then the eigenvectors and eigenvalues of a 3×3 absorption matrix which can be used to describe the absorption of light of arbitrary direction of propagation. The appropriate absorption matrix in the Cartesian basis $\hat{e}_1, \hat{e}_2$ for light propagating along $\hat{k}$ [see (17) and (18)] is obtained by inserting the relevant projection factors:

$$\begin{aligned}\mathscr{K}_{ij} &= \sum_{q=-1}^{+1} (\hat{e}_i\cdot\hat{\varepsilon}_q)\,\mathscr{K}_q\,(\hat{\varepsilon}_q^*\cdot\hat{e}_j) \qquad i, j = 1,2\,;\\ &= \begin{pmatrix} (\mathscr{K}_+ + \mathscr{K}_-)/2 & -i/2\cos\theta\,(\mathscr{K}_+ - \mathscr{K}_-) \\ i/2\cos\theta\,(\mathscr{K}_+ - \mathscr{K}_-) & \tfrac{1}{2}[(\mathscr{K}_+ + \mathscr{K}_-) + (2\mathscr{K}_0 - \mathscr{K}_+ - \mathscr{K}_-)\sin^2\theta] \end{pmatrix}.\end{aligned} \tag{21}$$

The values for the net circular and linear polarizations of the radiation emerging from the optically thin layer [see Equation (16)] are

$$\begin{aligned}\frac{v}{\delta s} &= -\tfrac{1}{2}(\mathscr{K}_+ - \mathscr{K}_-)\cos\theta\\ \frac{p_{\max}}{\delta s} &= \tfrac{1}{4}(2\mathscr{K}_0 - \mathscr{K}_+ - \mathscr{K}_-)\sin^2\theta.\end{aligned} \tag{22}$$

https://doi.org/10.1017/S0074180900100075 Published online by Cambridge University Press

The mean optical depth of the absorption layer is

$$\bar{\tau} \equiv \delta s \tfrac{1}{2} \operatorname{tr}(\mathscr{K}) = \delta s \left[(\mathscr{K}_+ + \mathscr{K}_-) \frac{1 + \cos^2\theta}{4} + \mathscr{K}_0 \frac{\sin^2\theta}{2} \right]. \tag{23}$$

3. Bound-Free Opacities in Magnetic Fields

In the previous section we obtained the form of the absorption matrix in the dipole approximation, and developed expressions for the Stokes polarization parameters for an optically-thin absorbing layer. A major contribution to the continuum opacity in cooler white dwarfs is the bound-free opacity. The dipole approximation is always fully justified in calculating the atomic bound-free opacity in the optical. Thus in the present section we analyze, within the hydrogenic approximation, the frequency and magnetic field strength dependence of the absorption coefficients defined in (19). Besides hydrogen and helium, it may be possible to discuss the behavior of the opacities of the heavier elements within this approximation, if they are sufficiently ionized (it has been suggested by Greenstein *et al.* (1971) that heavier elements may be present in the atmospheres of the white dwarfs showing continuum polarization as a result of convection from the interior). The bound-free absorption coefficient of helium at optical wavelengths is very well represented by the hydrogenic result. This is because the optical absorption and emission spectra are due to transitions involving a single electron in an excited state. The other electron remains in the tightly bound 1s state and its only effect, to a great precision, is to reduce the effective nuclear charge to a value $\sim +e$; thus the use of hydrogenic wavefunctions in this case is fully justified. As an example of the application of this analysis, the continuum polarization produced by bound-free transitions in hydrogen is considered in detail.

The bound-free opacity is given by the photoionization cross section: a bound electron of energy $-\mathrm{I}$ absorbs a photon of energy $\hbar\omega$ making a transition to a continuum state of energy $\hbar\omega - \mathrm{I}$. Whenever the initial and final state wave functions are sufficiently 'rigid' with respect to perturbation by the magnetic field (this condition will be made more precise in a moment), then we may obtain simple expressions for the continuum K_q in terms of the zero-field opacity. This may be seen as follows.

Consider first the bound electron wave function. We are interested in magnetic fields strong enough ($B \gtrsim 10^4$ G) that the Paschen-Back limit has been reached. If at the same time the magnetic field is sufficiently weak and the bound electron sufficiently tightly bound so that the quadratic Zeeman effect can be ignored, then, because the linear Zeeman Hamiltonian is diagonal, the initial state wave function is unchanged by the magnetic field ('rigidity' of the initial state wave function). In this case only the energy of the bound state changes, by $m_i \hbar \Omega_L$ where m_i is the initial state magnetic quantum number and $\Omega_L = eB/2mc$ is the Larmor frequency of the bound electron. Now, far from the atom the free electron state is greatly distorted by the magnetic field: the electron must spiral along the direction of the magnetic field. On the other hand, the behavior of the free electron wave function is only needed out to an atomic

distance of the order of the bound state radius, since the matrix element for photoionization is given by a weighted overlap of the bound electron and free electron wave functions. Thus, provided the kinetic energy of the free electron is sufficiently large, the magnetic field can again be treated in first order. If furthermore we work with eigenstates of L_z (the magnetic field being taken along the z-axis) then the free electron wave function – out to the radius of the bound state – may be approximated by the zero-field wave function, with the appropriate linear Zeeman shift $m_f \hbar\Omega_L$ in the energy ('rigidity' of the final state wave function).

The condition that the bound state quadratic Zeeman effect can be neglected in comparison to the linear Zeeman effect is

$$\frac{e^2 B^2 \langle r^2 \rangle}{8\, mc^2} \ll \hbar\Omega_L , \tag{24}$$

where r is the radius of the bound state wave function. For a bound state of principal quantum number n, (24) becomes

$$n^4 B_7 \ll 10^3 , \tag{25}$$

where B_7 is the magnetic field strength in units of 10^7 G. For Balmer and Paschen bound-free transitions in hydrogen ($n=2$ and $n=3$), (25) is still satisfied for $B=10^7$ G. The condition on the kinetic energy of the free electron is

$$\frac{p^2}{2m} \gg \frac{e^2 B^2}{8\, mc^2} \langle r^2 \rangle \tag{26}$$

or, equivalently,

$$\langle r^2 \rangle \ll r_L^2 , \tag{27}$$

where r is the radius of the bound state wave function and $r_L = v/\Omega_L$ is the Larmor radius of the electron in the magnetic field. From (24) and the condition (26) we see that for photoionization from a state of principal quantum number n, the first-order approximation will always fail in a wavelength interval

$$\Delta\lambda/\lambda = 4.53 \times 10^{-6} B_7^2 n^6 , \tag{28}$$

just above threshold. For the Balmer edge ($\lambda 3650$) and the Paschen edge ($\lambda 8201$), (28) gives $\Delta\lambda = 1.04$ Å and 27.1 Å, respectively, for $B=10^7$ G. As will be shown below, this wavelength interval is negligible compared to the interval over which interesting effects occur. It is clear that in the approximation which has just been described, the absorption coefficient for photoionization in the magnetic field can be written in terms of the zero-field absorption coefficient. We turn now to the details of this program.

For bound-free processes the largest contribution to the opacity is made in the vicinity of the absorption edge. In this region the photon wavelength is much greater than the radius of the bound state wave function for the cases being considered, so

that the dipole approximation is valid. Thus the bound-free absorption coefficients are given by (19):

$$\mathscr{K}_q = \text{const.} \times 4\pi^2 \frac{e^2\omega}{c} \sum_{i,f} |\langle f| d_q |i\rangle|^2 \delta(E_f - E_i - \hbar\omega), \quad q = 0, \pm . \tag{29}$$

Here $\hbar\omega$ is the photon energy, and $E_i (= -\mathrm{I})$ and E_f are, respectively, the energies of the bound and ionized electrons, including the linear interaction with the external magnetic field. The matrix elements of d_q in the rigid wave function approximation are easily evaluated in terms of the zero-field matrix elements: the wave functions are unchanged by the magnetic field while the energies of the initial and final states are shifted linearly with field strength (the difference in linear Zeeman shift is the same for all pairs of states connected by a given d_q, namely, $\hbar\Omega_L q$). Thus, if in the absence of a magnetic field

$$\sum_{i,f} |\langle f| d_q |i\rangle|^2 \delta(E_f - E_i - \hbar\omega) = f_q(\omega), \tag{30}$$

then with a magnetic field present

$$\sum_{i,f} |\langle f| d_q |i\rangle|^2 \delta(E_f - E_i - \hbar\omega) = f_q(\omega - q\Omega_L). \tag{31}$$

The function f_q in (30) and (31) must be the same for all q, since only in this case will the zero-field absorption coefficient be independent of q, as required. Thus the absorption coefficients are given by

$$\mathscr{K}_q(\omega) = \text{const.}\ \omega f(\omega - q\Omega_L), \tag{32}$$

and these may be put directly into (22) and (23) to obtain the circular and linear polarization and mean optical depth for the optically thin absorption layer:

$$\begin{aligned}
\frac{v(\theta)}{\bar{\tau}} &= -\frac{[f(\omega - \Omega_L) - f(\omega + \Omega_L)]\cos\theta}{[f(\omega - \Omega_L) + f(\omega + \Omega_L)]\,(1 + \cos^2\theta)/2 + f(\omega)\sin^2\theta} \\
\frac{p_{\max}(\theta)}{\bar{\tau}} &= -\frac{[f(\omega) - 1/2(f(\omega - \Omega_L) + f(\omega + \Omega_L))]\sin^2\theta}{[f(\omega - \Omega_L) + f(\omega + \Omega_L)]\,(1 + \cos^2\theta)/2 + f(\omega)\sin^2\theta} \\
\bar{\tau} &= \frac{\delta s}{2}\left[(\mathscr{K}_+ + \mathscr{K}_-)\frac{(1 + \cos^2\theta)}{2} + \mathscr{K}_0 \sin^2\theta\right].
\end{aligned} \tag{33}$$

If $\Omega_L/\omega \ll 1$ and f is smoothly varying, then we may expand $f(\omega \pm \Omega_L)$ in a Taylor series with the result, to lowest order in Ω_L/ω,

$$\begin{aligned}
\frac{v(\theta)}{\bar{\tau}} &= \left(\frac{\Omega_L}{\omega}\right)\cos\theta\left[\frac{\omega}{f(\omega)}\frac{\mathrm{d}f(\omega)}{\mathrm{d}\omega}\right] \\
\frac{p_{\max}}{\bar{\tau}} &= \left(\frac{\Omega_L}{\omega}\right)^2 \frac{\sin^2\theta}{4}\left[\frac{\omega^2}{f(\omega)}\frac{\mathrm{d}^2 f(\omega)}{\mathrm{d}\omega^2}\right].
\end{aligned} \tag{34}$$

In (34) it has been assumed that $(\Omega_L^2/f)\,\mathrm{d}^2 f/\mathrm{d}\omega^2 \ll 1$.

https://doi.org/10.1017/S0074180900100075 Published online by Cambridge University Press

Let us turn now to a specific bound-free opacity, that of hydrogen. Let $\bar{\sigma}_n$ be the absorption cross section per electron in an energy level of principal quantum number n, averaged over the orbital angular momentum quantum numbers (see Frank-Kamenetskii, 1962). For light of wavelength $\lambda \lesssim 15000$ Å we need only consider photoionization from levels with $n \leqslant 4$. Then the function $f(\omega)$ defined by (30) is given by

$$f(\omega) = \frac{1}{\omega}\sigma(\omega) \simeq \frac{1}{\omega}\sum_{n=1}^{4} \bar{\sigma}_n(\omega). \tag{35}$$

Figure 3(a) indicates the general behavior (although much exaggerated) of the absorption coefficients $K_q(\omega)$. The resulting net polarizations $v/\bar{\tau}$ and $p_{\max}/\bar{\tau}$ (the former calculated for propagation along the field and the latter, for propagation normal to the field) are shown in Figure 3(b) for a field of 10^7 G. As an example of the behavior of the polarization near an absorption edge, the frequency dependence of $v/\bar{\tau}$ and $p_{\max}/\bar{\tau}$ of the Balmer edge is shown in greater detail in Figure 3(c).

Except near the absorption edges, $v/\bar{\tau}$ and $p_{\max}/\bar{\tau}$ are well-represented by the functions

$$\frac{v(\theta)}{\bar{\tau}} = -4\left(\frac{\Omega_L}{\omega}\right)\cos\theta \quad \text{and} \quad \frac{p_{\max}(\theta)}{\bar{\tau}} = 5\left(\frac{\Omega_L}{\omega}\right)^2 \sin^2\theta. \tag{36}$$

These results may be understood by recalling that the Kramers approximation to the bound-free opacity, which is accurate over a wide range of frequencies, gives $\bar{\sigma}_n = \text{const.}\ n^{-5}\omega^{-3}$ or $f(\omega) \sim \omega^{-4}$. In this approximation (34) gives exactly the result (36). We may remark that in the wavelength intervals where (36) is valid (away from the absorption edges), the hydrogen bound-free opacity gives, for an optically thin absorbing layer, the same field strength and frequency dependence as the grey-body model.

The relation between the bound-free case discussed here and the grey-body case discussed by Kemp can be seen from (35). In the greybody case, $\sigma(\omega) = \text{const.}$ by definition, so that $f(\omega) = (\text{const.})\,\omega^{-1}$. This gives the same behavior as that obtained here for the bound-free case, except, of course, near an absorption edge.

Near an absorption edge the cross section is discontinuous, and the polarization is given by (33). The result is that $v/\bar{\tau}$ changes sign and becomes large in the interval $\lambda_- \leqslant \lambda \leqslant \lambda_+$, where

$$\lambda_\pm = \lambda_0\,(1 \mp \lambda_0/\lambda_L)^{-1} \tag{37}$$

in terms of the wavelength λ_0 of the absorption edge in zero field and $\lambda_L \equiv 2\pi c/\Omega_L$. For a field of 10^7 G, this interval extends for ~ 60 Å on either side of the Balmer edge ($\lambda 3646$) and for ~ 300 Å on either side of the Paschen edge ($\lambda 8201$). In these same intervals $p_{\max}/\bar{\tau}$ also becomes large and changes sign twice. The magnitudes of $v/\bar{\tau}$ and $p_{\max}/\bar{\tau}$ are independent of field strength in the intervals $\lambda_- \leqslant \lambda \leqslant \lambda_+$. The values of $v/\bar{\tau}$ and $p_{\max}/\bar{\tau}$ in these intervals may be estimated quite accurately by again using

https://doi.org/10.1017/S0074180900100075 Published online by Cambridge University Press

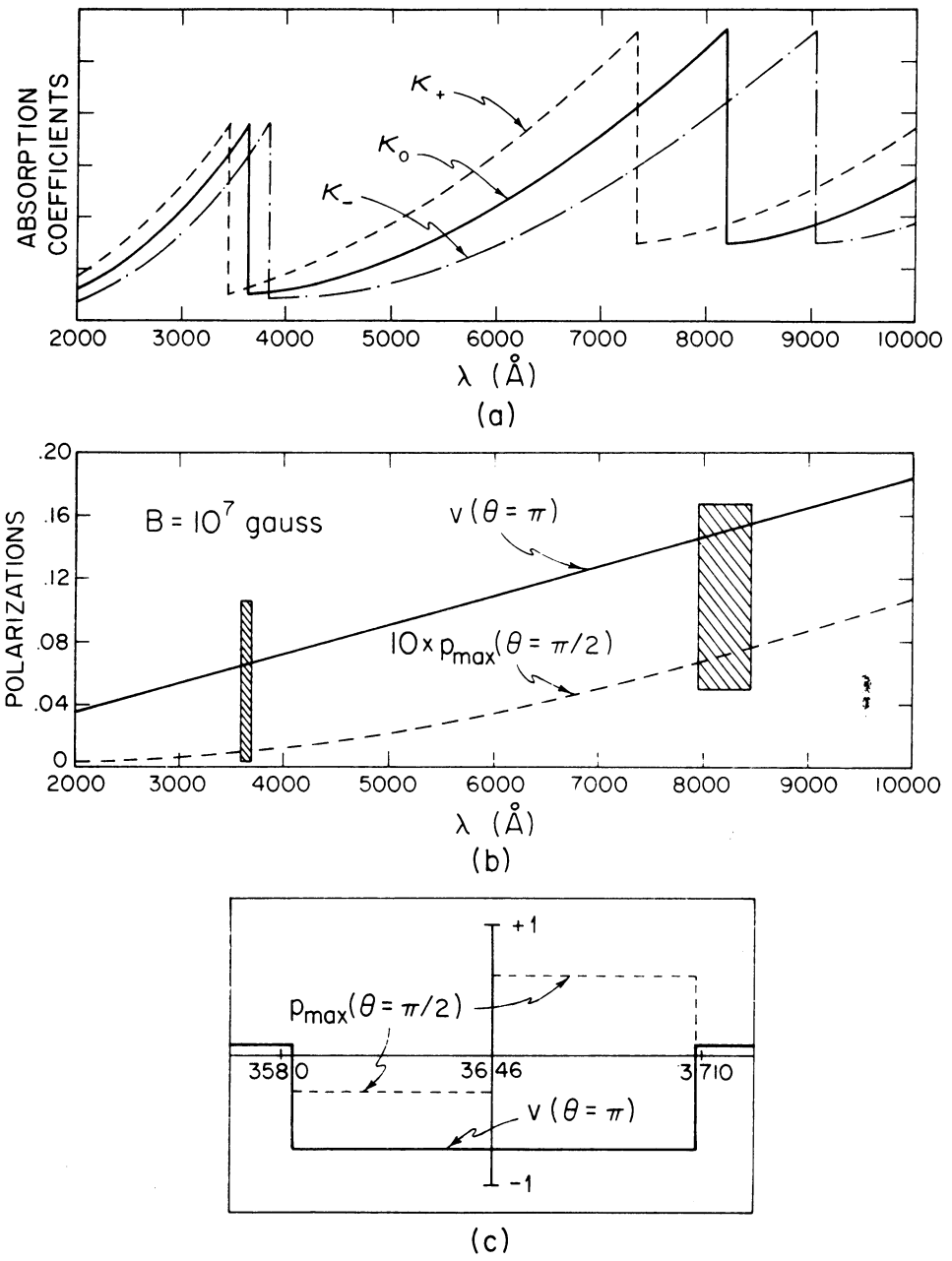

Fig. 3. The behavior of the absorption coefficients for bound-free absorption in a magnetic field and the resulting circular and linear continuum polarization. The general behavior of the absorption coefficients is shown in (a), although much exaggerated. The resulting net polarizations $v/\bar{\tau}$ and $p_{max}/\bar{\tau}$, calculated for propagation parallel and perpendicular to the field, respectively, are shown in (b) for $B = 10^7$ G. The detailed behavior of $v/\bar{\tau}$ and $p_{max}/\bar{\tau}$ at the Balmer edge is shown in (c).

https://doi.org/10.1017/S0074180900100075 Published online by Cambridge University Press

the Kramers approximation. At the Balmer edge this gives

$$\frac{v(\theta=\pi)}{\bar{\tau}} \simeq -0.77 \qquad 3586\ \text{Å} \lesssim \lambda \lesssim 3706\ \text{Å}$$

and

$$\frac{p_{\max}(\theta=\pi/2)}{\bar{\tau}} \simeq \begin{cases} -0.28 & 3586\ \text{Å} \lesssim \lambda < 3646\ \text{Å} \\ +0.62 & 3646\ \text{Å} < \lambda \lesssim 3706\ \text{Å}, \end{cases}$$

while at the Paschen edge we have

$$\frac{v(\theta=\pi)}{\bar{\tau}} \simeq -0.62 \qquad 7900\ \text{Å} \lesssim \lambda \lesssim 8500\ \text{Å}$$

$$\frac{p_{\max}(\theta=\pi/2)}{\bar{\tau}} \simeq \begin{cases} -0.24 & 7900\ \text{Å} \lesssim \lambda < 8201\ \text{Å} \\ +0.45 & 8201\ \text{Å} < \lambda \lesssim 8500\ \text{Å}. \end{cases}$$

By contrast, a field of 10^7 G gives $v(\theta=\pi)/\bar{\tau}=0.073$ and $p_{\max}(\theta=\pi/2)/\bar{\tau}=0.0017$ at $\lambda 4000$, far from the edges. The Balmer edge behavior is illustrated in Figure 3(c). The behavior near the Balmer edges of helium is somewhat more complicated. Because the effective screening of the nucleus by the $1s$ electron depends somewhat upon the orbital angular momentum of the outer electron and the total spin of the two electrons, there are four separate Balmer edges (two each for orthohelium and parahelium). These edges appear at $\lambda\lambda 2600$, 3420 in orthohelium and at $\lambda\lambda 3120$, 3680 in parahelium – in both cases the separation between the edges considerably exceeds the width of the region of characteristic polarization changes, even for field strengths as great as 10^7 G. For higher wavelength edges in helium the situation simplifies because the screening of the nucleus varies less with the angular momentum states.

If some white dwarfs have magnetic fields as large as $B \sim 10^7$ G and if photoionization of hydrogen-like atoms is a significant source of opacity, then features of the type just described should be observable near absorption edges. It must be kept in mind, however, that disordered fields and the presence of other opacity sources will tend to wash out these features to a greater or lesser degree, depending on the structure of the atmosphere.

4. Free-Free Absorption in Magnetic Fields

In normal white dwarf atmospheres, an important contribution to the continuum opacity is due to free-free absorption by electrons moving in the Coulomb field of ions (inverse bremsstrahlung). In the presence of a magnetic field a new type of process becomes possible in which electrons which are otherwise free are able to absorb radiation by transferring momentum to the magnetic field (the inverse of cyclotron radiation). This process will give rise to a continuous opacity with a strong linear and circular absorption peak near the cyclotron resonance frequency, $\Omega_c = eB/mc$, corresponding to transitions between adjacent Landau levels. For magnetic field strengths $B \gtrsim 10^8$ G, this peak will fall in the infrared or optical (the wavelength in

https://doi.org/10.1017/S0074180900100075 Published online by Cambridge University Press

μm is $\lambda_c = 2\pi c/\Omega_c = 1.07/B_8$, where B_8 is the field strength in units of 10^8 G). For this reason, it has been suggested (see Kemp, 1970b) that the cyclotron process may be related to the polarization features seen in the white dwarf Grw+70°8247. In the present section we obtain a quantitative estimate for the free-free opacity in magnetic white dwarf atmospheres due to this process and compare it with the results for the bound-free opacity obtained in the previous section.

For the temperatures typical of white dwarf atmospheres ($T \sim 10^4$K) and the magnetic field strengths of interest ($B \sim 10^8$ G), $\hbar\Omega_c \sim k_B T$ so that only the first few Landau levels will be significantly populated. Thus the cyclotron absorption cross section must be calculated quantum-mechanically. The cyclotron radius of the electron motion, for magnetic fields of these strengths and velocities determined by these temperatures, is considerably smaller than the wavelength of radiation at the cyclotron frequency. As a consequence the absorption of radiation is governed by the usual electric dipole rules, and we may thus calculate the opacities $K_q = n_e \sigma_q$ defined in (19). Here n_e is the number density of free electrons. In addition, the spiral-like motion of the electrons provides the kinematic restrictions that σ_-, σ_0 are negligible while σ_+ is peaked at the cyclotron frequency. Assuming nondegenerate electrons in LTE, the absorption cross section σ_+ is (see Lamb and Sutherland, 1971):

$$\sigma_+(\omega, \theta) \approx \frac{1}{|\cos\theta|} \frac{1}{\sqrt{\pi}} \left(\frac{e^2}{\hbar c}\right) \left(\frac{2\pi c}{\Omega_c}\right)^2 \left(\frac{mc^2}{2k_B T}\right)^{1/2} \times \times \left(\frac{B}{B_q}\right) \frac{1}{1 - e^{-\hbar\Omega_c/k_B T}} \exp\left\{-\frac{mc^2}{2k_B T \cos^2\theta} \frac{(\omega - \Omega_c)^2}{\Omega_c^2}\right\}, \quad (38)$$

for light of angular frequency ω propagating at an angle θ with respect to the magnetic field; here $B_q = m^2 c^3/e\hbar = 4.414 \times 10^{13}$ G. From (38) it is evident that the cross section is strongly peaked about $\omega = \Omega_c$ with a width given by

$$\frac{\Delta\omega}{\Omega_c} \approx \left(\frac{2k_B T}{mc^2}\right)^{1/2} |\cos\theta| . \quad (39)$$

A measure of the strength of the absorption is provided by the frequency-integrated cross section:

$$\sigma_+ \equiv \int d\omega\, \sigma_+(\omega, \theta) \approx \frac{e^2}{\hbar c} \left(\frac{2\pi c}{\Omega_c}\right)^2 \left(\frac{B}{B_q}\right) \frac{\Omega_c}{1 - e^{-\hbar\Omega_c/k_B T}} . \quad (40)$$

For $T = 10^4$ K and $B = 10^8$ G, the peak occurs at $\lambda 10700$ with a full width at $1/e$ of roughly 39 $|\cos\theta|$ Å (cf. Figure 4); (40) gives for the integrated cross section 0.45 cm^2 s^{-1}. By comparison, the frequency-integrated cross section for hydrogen bound-free absorption from the Paschen edge to the Balmer edge is only 0.02 cm^2 s^{-1}.

Because only one K_q (that for $q = +1$) is nonzero, the light in the neighborhood of the cyclotron absorption feature should exhibit strong circular and linear polarization. For the sake of comparison with the results of Section 3, we may note that a homogeneous magnetic field in a layer of optical depth $\bar{\tau} \ll 1$ whose opacity is due

only to cyclotron absorption will lead to values of $v(\theta)/\bar{\tau}$ and $p_{\max}(\theta)/\bar{\tau}$ [cf. (22) and (23)] given by

$$\frac{v(\theta)}{\bar{\tau}} = -\frac{2\cos\theta}{1+\cos^2\theta}, \qquad \frac{p_{\max}}{\bar{\tau}} = \frac{\sin^2\theta}{1+\cos^2\theta}, \tag{41}$$

where θ is the angle between the direction of propagation and the magnetic field; of course these polarizations only exist in the immediate vicinity of the cyclotron frequency [cf. (39)]. Both v and $p_{\max}$ have the same sign as given by absorption due to hydrogen-like bound-free transitions at wavelengths not in the vicinity of an absorption edge.

In a typical white dwarf atmosphere, the magnetic field is expected to be far from uniform – it will vary both in magnitude and direction over the stellar surface. The effect of variations in magnitude is to shift the location of the cyclotron absorption peak. Thus at a particular frequency one observes (due to the cyclotron absorption)

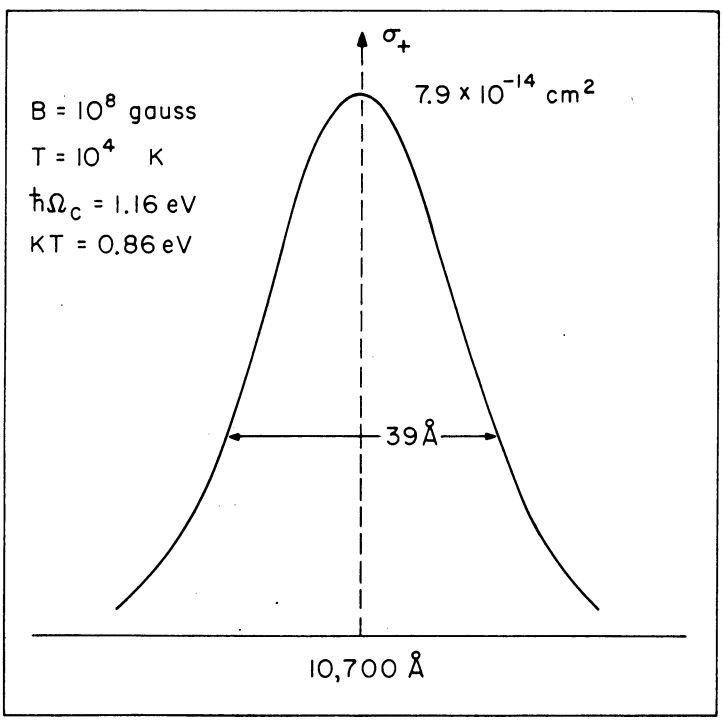

Fig. 4. Characteristics of the cyclotron absorption cross section σ_+ for the indicated temperature and magnetic field. The width shown is the full width at $\sigma_+(\max)/e$.

https://doi.org/10.1017/S0074180900100075 Published online by Cambridge University Press

contributions to the polarization from all points in the stellar atmosphere for which the magnetic field strength is (roughly) the same; for these points, however, the angle θ between the magnetic field and light propagating towards the observer will in general vary so that v and $p_{\max}$ as given in (41) must be suitably averaged.

5. Conclusions

In the preceding sections we have presented some of the effects magnetic fields in the range 10^4–10^8 G would have on the observed continuum emission of white dwarfs. Before examining the magnetic field effects at the atomic level, we introduced the radiative transfer equation for polarized light in an anisotropic medium. Within this framework it is possible to discuss the relative effects of the real and imaginary parts of the indices of refraction of the medium, to obtain the form of the emission matrix, and to isolate the geometrical factors related to the direction of propagation of the light relative to the magnetic field. We found that in a semi-infinite plane-parallel atmosphere, provided the characteristic states of the medium are nearly orthogonal, the polarization of the radiation is determined only by the absorption matrix and the run of temperature in the atmosphere. For the case of electric dipole absorption in a magnetic field the absorption matrix may be directly expressed in terms of the atomic absorption coefficients and the geometrical factors. To illustrate the qualitative features of the polarization induced by such anisotropic absorption, we considered absorption by a cold, optically-thin layer. In this greatly simplified model of a white dwarf atmosphere, we obtained formulae for the net circular and linear polarizations in terms of the absorption coefficients and the geometrical factors.

The continuum polarization arising from bound-free transitions in magnetic fields was calculated within the hydrogenic approximation. Away from absorption edges a hydrogenic bound-free opacity gives the same field strength and frequency dependence of the polarizations as that given by the grey-body model. However, near an absorption edge the opacity is discontinuous and the polarization undergoes sudden changes in sign and magnitude. If hydrogen or helium bound-free processes (or those of heavier atoms satisfying the hydrogenic approximation) form a significant source of opacity in white dwarfs with magnetic fields of order 10^7 G, these changes should be observable. Discovery of this type of behavior in the continuum polarization of white dwarfs would be of great interest for at least two reasons. First, it would indicate that a particular bound-free opacity makes a significant contribution to the star's opacity, thus yielding information about the composition, density, and temperature of the atmosphere. In this connection it is worth noting that fields as large as 10^7 G might make difficult the detection of an absorption edge using intensity measurements alone. Second, it would make possible a more accurate estimate of the average field strength than is possible on the basis of broad-band continuum polarization measurements. For these reasons, a search for edge behavior in the continuum polarization of white dwarfs seems desirable.

We have also discussed the opacity due to cyclotron absorption by electrons. The

cross section is strongly peaked at the cyclotron frequency, which falls in the infrared or optical for $B \geqslant 10^8$ G, and is large (the integrated cyclotron cross section is $\sim 10^2$ times the hydrogen bound-free absorption cross section integrated over the optical region of the spectrum). This process can produce net linear and circular polarizations of comparable magnitude. For stars with magnetic fields that are not constant in magnitude and direction throughout the atmosphere, the cyclotron absorption effects will be spread across considerable wavelength ranges with possibly quite complicated wavelength-dependent polarizations.

Acknowledgements

We are grateful to many colleagues, both at Columbia and the University of Illinois, for many fruitful discussions, and to Roger Angel for communicating in advance of publication details of work performed by him and Landstreet. We would like to express appreciation for the kind hospitality of the Aspen Center for Physics, where part of this work was completed. This work was supported by NSF Grants GP25855 and GP32336X.

Appendix

In this appendix we discuss the polarization information contained in the polarization matrix and give rules for the determination of the Stokes parameters (further details may be found in Lamb and ter Haar (1970)). The polarization matrix is in most respects similar to the density matrix introduced in quantum mechanics; the primary difference is that the polarization matrix does not have a fixed normalization, in order that the absorption of light as it propagates through the medium may be represented within the polarization matrix formalism.

The polarization matrix in the Cartesian basis, $\mathscr{I}^{(c)}$, is Hermitian and thus its eigenvectors may be chosen to form an orthonormal basis. The congruency transformation of $\mathscr{I}^{(c)}$ under this change of orthonormal bases diagonalizes the polarization matrix:

$$\mathscr{I}' = \mathscr{U}^{-1}\mathscr{I}^{(c)}\mathscr{U}^{-1\dagger} = \begin{pmatrix} \lambda_+ & 0 \\ 0 & \lambda_- \end{pmatrix}. \tag{A1}$$

The degree of polarization p is given by

$$p = \frac{\lambda_+ - \lambda_-}{\lambda_+ + \lambda_-} \tag{A2}$$

from which it follows that p may be written in the invariant form

$$p = \left\{1 - \frac{4 \det(\mathscr{I})}{[\mathrm{tr}(\mathscr{I})]^2}\right\}^{1/2}. \tag{A3}$$

Because the transformation of the polarization matrix under a change of basis from the Cartesian basis [see (3) and (4)] is only a similarity transformation if the new basis

is orthonormal, we must restrict ourselves to orthonormal bases so that the trace and determinant of the polarization matrix have invariant values. The trace of $\mathscr{I}$ is just the net intensity of the radiation; det $(\mathscr{I})=0$ is a necessary and sufficient condition for the radiation to be completely polarized. Note that unpolarized radiation is characterized by a polarization matrix proportional to the unit matrix, the proportionality constant being one-half the total intensity.

Various sets of Stokes parameters may be introduced to give an alternative description of polarized radiation (see, for example, Chandrasekhar, 1960, pp. 24–31); these may, in general, be obtained from the polarization matrix in the Cartesian basis. A conventional set of Stokes parameters is given by:

$$S_i = \mathrm{tr}\,(\sigma_i \mathscr{I}^{(c)}) \qquad i = 0, 1, 2, 3 \tag{A4}$$

where the σ_i are the Pauli matrices and the unit matrix:

$$\sigma_0 = \begin{pmatrix} 1 & 0 \\ 0 & 1 \end{pmatrix}, \quad \sigma_1 = \begin{pmatrix} 1 & 0 \\ 0 & -1 \end{pmatrix}, \quad \sigma_2 = \begin{pmatrix} 0 & 1 \\ 1 & 0 \end{pmatrix}, \quad \sigma_3 = \begin{pmatrix} 0 & -i \\ i & 0 \end{pmatrix}. \tag{A5}$$

S_0 is the net intensity and one may easily show that $v = S_3/S_0$ is the net circular polarization. The net linear polarization along an axis inclined at an angle ϕ to the 1-axis (the light propagates along the 3-axis), defined as the linear polarization measured along this axis minus the linear polarization measured along an axis at right angles to this axis, is given by

$$\begin{aligned} p(\phi) &\equiv p_{\parallel} - p_{\perp} \\ &= (S_1 \cos 2\phi + S_2 \sin 2\phi)/S_0 . \end{aligned} \tag{A6}$$

The quantity $p_{\max}$ appearing in the previous sections and referred to as the 'net linear polarization' is the maximum value of $p(\phi)$ with respect to ϕ. It is conventional to choose the (as yet unspecified) orientation of the Cartesian 1-axis so that $p_{\max}$ coincides with S_1/S_0.

References

Angel, J. R. P.: 1972, *Astrophys. J. Letters* **171**, L17.
Angel, J. R. P. and Landstreet, J. D.: 1970a, *Astrophys. J. Letters* **160**, L147.
Angel, J. R. P. and Landstreet, J. D.: 1970b, *Astrophys. J. Letters* **162**, L61.
Angel, J. R. P. and Landstreet, J. D.: 1971a, *Astrophys. J. Letters* **164**, L15.
Angel, J. R. P. and Landstreet, J. D.: 1971b, *Astrophys. J. Letters* **165**, L71.
Angel, J. R. P. and Landstreet, J. D.: 1972, *Astrophys. J. Letters*, **178**, L21.
Angel, J. R. P., Illing, R. M. E., and Landstreet, J. D.: 1972a, *Astrophys. J. Letters* **175**, L85.
Angel, J. R. P., Landstreet, J. D., and Oke, J. B.: 1972b, *Astrophys. J. Letters* **171**, L11.
Chandrasekhar, S.: 1960, *Radiative Transfer*, Dover, New York, p. 24ff.
Chanmugam, G., O'Connell, R. F., and Rajagopal, A. K.: 1972, *Astrophys. J.* **175**, 157.
Chow, T. L.: 1969, *Astrophys. Letters* **3**, 85.
Frank-Kamenetskii, D. A.: 1962, *Physical Processes in Stellar Interiors* (translated from the Russian and published for the National Science Foundation by the Israel Program for Scientific Translations), p. 144.
Gehrels, T.: 1971 (unpublished).
Ginzburg, V. L., Zheleznyakov, V. V., and Zaitsev, V. V.: 1969, *Astrophys. Space Sci.* **4**, 464.
Greenstein, J. L.: 1970, *Astrophys. J. Letters* **162**, L55.

Greenstein, J. L., Gunn, J. E., and Kristian, J.: 1971, *Astrophys. J. Letters* **169**, L63.
Greenstein, J. L. and Matthews, M. S.: 1957, *Astrophys. J.* **126**, 14.
Kemp, J. C.: 1970a, *Astrophys. J. Letters* **162**, L69.
Kemp, J. C.: 1970b, *Astrophys. J.* **162**, 169.
Kemp, J. C. and Swedlund, J. B.: 1970, *Astrophys. J. Letters* **162**, L67.
Kemp, J. C., Swedlund, J. B., Landstreet, J. D., and Angel, J. R. P.: 1970, *Astrophys. J. Letters* **161**, L77.
Kemp, J. C., Swedlund, J. B., and Wolstencroft, R. D.: 1971, *Astrophys. J. Letters* **164**, L17.
Lamb, F. K. and ter Haar, D.: 1970, Oxford University, Department of Theoretical Physics, Reference No. 38/70.
Lamb, F. K. and Sutherland, P. G.: 1971, paper presented at the Conference on Line Formation in the Presence of Magnetic Fields, 30 August–2 September 1971, High Altitude Observatory, Boulder, Colorado.
Landstreet, J. D. and Angel, J. R. P.: 1971, *Astrophys. J. Letters* **165**, L67.
Ostriker, J. P. and Hartwick, F. D. A.: 1968, *Astrophys. J.* **153**, 797.
Preston, G. W.: 1970, *Astrophys. J. Letters* **160**, L143.
Shipman, H. L.: 1971, *Astrophys. J.* **167**, 165.
Trimble, V.: 1971, *Nature* **231**, 124.